ELSEVIER

Chemical Engineering Journal 84 (2001) 95–105

Chemical Engineering Journal

www.elsevier.com/locate/cej

Adsorption kinetics for the removal of chromium(VI) from aqueous solution by adsorbents derived from used tyres and sawdust

Nadhem K. Hamadi [a,*], Xiao Dong Chen [a], Mohammed M. Farid [a], Max G.Q. Lu [b]

[a] *Department of Chemical and Materials Engineering, The University of Auckland, Private Bag 92019, Auckland, New Zealand*

[b] *Department of Chemical Engineering, University of Queensland, Brisbane, Qld, Australia*

Abstract

The batch removal of hexavalent chromium (Cr(VI)) from wastewater under different experimental conditions using economic adsorbents was investigated in this study. These adsorbents were produced from the pyrolysis and activation of the waste tyres (TAC) and from the pyrolysis of sawdust (SPC). The performance of these adsorbents against commercial activated carbon F400 (CAC) has also been carried out. The removal was favoured at low pH, with maximum removal at pH = 2 for all types of carbon. The effects of concentration, temperature and particle size have been reported. All sorbents were found to efficiently remove Cr(VI) from solution.

The batch sorption kinetics have been tested for a first-order reversible reaction, a first-order and second-order reaction. The rate constants of adsorption for all these kinetic models have been calculated. The applicability of the Langmuir isotherm for the present system has been tested at different temperatures. The thermodynamic parameters (ΔG^0, K_c) obtained indicate the endothermic nature of Cr(VI) adsorption on TAC, SPC and CAC.

Keywords: Used tyres; Sawdust; Pyrolysis; Activation; Adsorption kinetics; Langmuir isotherm; Hexavalent chromium; Thermodynamic parameters

1. Introduction

The disposal of used tyres is becoming a serious environmental issue. An estimated 1.5×10^6, 2.5×10^6 and 0.5×10^6 tonnes of used tyres are generated each year in European Community, North America and Japan, respectively [1]. The majority of this tyre waste is dumped in open dumping or landfill sites. However, tyres do not degrade in landfills and open dumping may result in accidental fires with high pollution emissions. In addition this route of disposal ignores, the large energy potential of used tyres. Incineration has been considered as an alternative to dumping in an effort to utilise the high calorific value of used tyres, but this proposal may not maximise the potential economic recovery of energy and chemical materials from the waste. Pyrolysis of tyres to produce liquid hydrocarbons and gases is currently receiving renewed attention, since the derived products are easily handled, stored and transported and hence do not have to be used at or near the recycling plant. The derived oils may be used directly as fuel or added to petroleum refinery feed stocks. The oil may also be an important source of refined chemicals, since it has been shown that they contain high concentration of potentially valuable chemical feed stocks, for example, benzene, toluene and xylene according to Roy and Unsworth [2]. The derived gases are also useful as fuel and the solid char may be used either as smokeless fuel, carbon black or activated carbon.

In previous tyre pyrolysis studies, e.g. Schulman and White [3], Kaminsky and Sinn [4], Kaminsky and Rossler [5] and Merchant and Petrich [6], the quantity of char has been found to exceed the amount of carbon black present in the used tyres. Thus, the solid product may be regarded as a mixture of carbon black and char formed by tyre rubber degradation. The economic feasibility of tyre pyrolysis is strongly affected by the value of this solid pyrolysis residue. In this study, the ability of pyrolysed tyres and sawdust to remove hexavalent chromium (Cr(VI)) from aqueous solution has been investigated.

Adsorption processes for water treatment have had a long and productive history. Early application of carbon in a water treatment plant to remove chloropheolic tastes was reported by Baylis in 1929 as summarised by Faust and Aly [7]. Activated carbon has been widely used in wastewater treatment to remove organic and inorganic pollutants. It was also found that activated carbon has a great potential to remove heavy metals such as cadmium, chromium and lead according to McKay et al. [8].

* Corresponding author. Tel.: +64-9-3737599; fax: +64-9-3737463.
E-mail addresses: n.hamadi@auckland.ac.nz (N.K. Hamadi), d.chen@auckland.ac.nz (X.D. Chen).

1385-8947/01/$ – see front matter
PII: S1385-8947(01)00194-2

Activated carbon frequently exhibits high removal efficiency for most dissolved components. The removal efficiency is influenced by the characteristics of the activated carbon produced. In general, the manufacturing processes determine the characteristics of the activated carbon produced. Depending on the nature of raw materials, the nature of activating agent and the conditions of activation process, the properties of the activated carbon can be varied. Selomulya et al. [9] have studied the removal mechanism of Cr(VI) from wastewater using activated carbon and they stated that removal efficiency was dependent on surface area and surface chemistry. Generally, activated carbon of higher surface area has high adsorption capacity. However, for the removal of dissolved metal ions, the surface properties also play an important role.

Heavy metals are widely used by modem industries, including textile, leather, tanning, electroplating and metal finishing. They are released to environment either in treated wastewater to surface waters or as sludge applied to landfill. Hexavalent chromium is known to be a strong oxidant. Because of its high toxicity, it is imperative to significantly reduce its discharge levels [10].

Previously, we studied the removal of Cr(VI) and colour (methylene blue) from wastewater, using adsorbents produced from waste tyres and sawdust under selected conditions [11,12]. These were preliminary studies. In this research, we investigate the adsorption kinetics of these adsorbents under wide range of conditions. In addition, a well-known standard activated carbon F400 was used as a reference.

2. Experimental

2.1. Materials preparation and characterisation

Pyrolysis was carried out in an isothermal reactor heated by a tubular furnace (i.d. = 61 mm, L = 55 cm). Fig. 1 shows the schematic diagram of the set-up. At the beginning of each run, 100 g of small pieces (3 cm × 2.5 cm × 0.5 cm) of used tyres were placed in a steel reactor tube (o.d. = 44 mm, L = 24.5 cm) supported on a 1-mm mesh located in the middle of the longer steel tube (o.d. = 60 mm, L = 79 cm). High purity nitrogen was used as the purging gas flowing through the sample bed at 200 ml/min. The reactor was then heated to the desired temperature (900°C) at a heating rate of 20°C/min and a holding time of 2 h. After the pyrolysis process, the product was activated at the same temperature for 2 h by using CO_2 as an oxidising agent. Then the reactor was cooled down to room temperature before the sample was removed for weighing and characterisation. The sawdust was pyrolysed at 650°C using the same set-up and the same time periods described above.

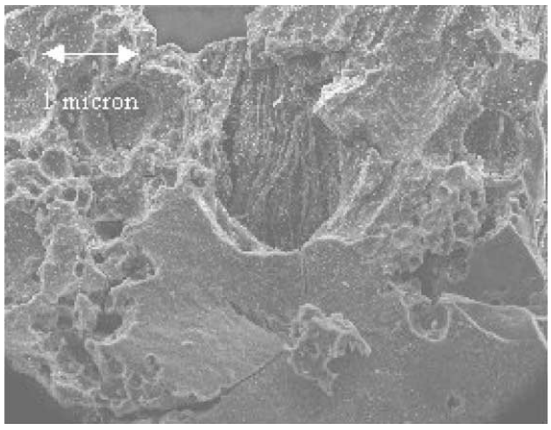

Fig. 2. SEM image of pyrolysed used tyres sample.

The adsorbents made in this work were characterised by scanning electron microscope (SEM) (see Figs. 2–4). These figures show that the two adsorbents have an irregular and porous surface, which indicates high surface areas. This conclusion has been proven by the BET surface area measurements, which show that the surface area of the activated carbon from the used tyre is 832 m^2/g and the surface area of the pyrolysed sawdust is 320 m^2/g.

Tests were performed on the TAC to determine the composition and physical properties of the carbon. The results of these tests are shown in the sections below. A Phillips PW 1050 X-ray diffractometer was used to carry out the test. The results of the X-ray diffraction confirm that the tyre activated does not have a crystalline structure. With no atomic lattice there are no characteristic peaks and hence

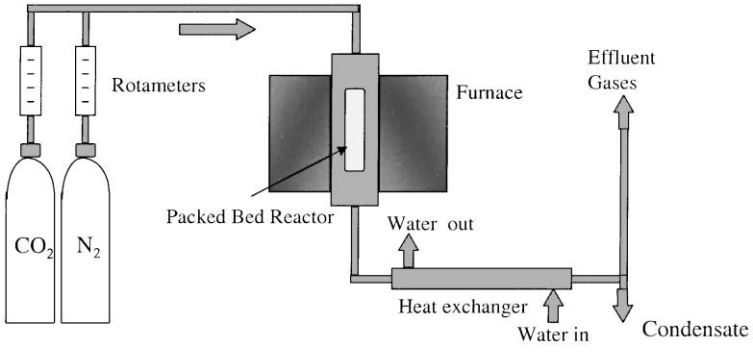

Fig. 1. Schematic diagram of the pyrolysis and activation process.

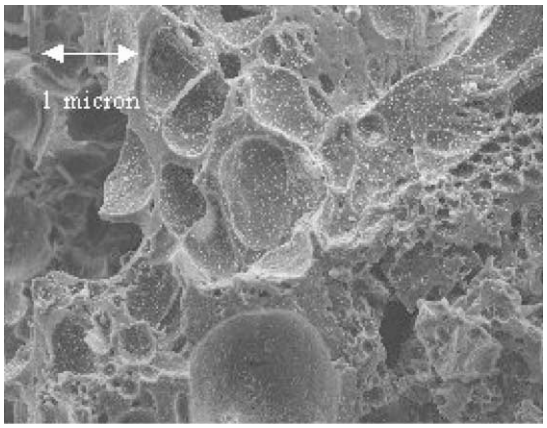

Fig. 3. SEM image of activated used tyres (TAC) sample.

the inconclusive results, the structure of the carbon is most likely amorphous.

Energy dispersive spectrometer (EDS) was also used to analyse tyre product. Tyres are primarily composed of vulcanised rubber, rubberised fabric containing reinforcing textile cords, steel or fabric belts and steel-wire reinforced rubber heads, Wojtowicz and Serio [13]. Styrene-butadiene rubber (SBR) is still the most important synthetic rubber used in the industry today although natural rubber is also used in tyres to some degree. Carbon black, extender oil, sulphur, zinc oxide and stearic acid are also added. Carbon black is used to strengthen the rubber and to improve its abrasion resistance. The bulk of a tyre is organic and carbonaceous in nature thus provides an ideal source for the production of activated carbon, Kim [14]. The EDS analysis provided a rudimentary composition for the tyre activated carbon. The compositions from the peak areas are calculated as shown in Table 1.

It was found that carbon, sulphur and oxygen were the only consistent components in the TAC. Other minor constituents that were obtained from the analyses included sodium, silicon, zinc, sodium, calcium, iron and vanadium.

The origins of the extra constituents in the carbon can be determined by considering the process and materials used in tyre manufacture. The sulphur is a result of the vulcanisation process. Many of the heavy metals are added to the tyre for strength or are naturally present in the long-chained organic components that rubber is composed of.

Table 1
EDS composition of TAC

Element	Weight (%)
Carbon	96.86
Oxygen	2.03
Sulphur	1.39

2.2. Adsorption

The measurement of adsorption kinetics of the carbon was carried out by shaking 0.4 g of carbon with 200 ml of Cr(VI) solution of known concentration in 250 ml conical flask placed in a thermostat provided with a shaking mechanism. The removal kinetics of the Cr(VI) was investigated by drawing samples after the desired contact time and the filtrate was analysed for the remaining Cr(VI) concentration. A spectrophotometer was employed at a wavelength of 540 nm with 1,5-diphenyl carbazide reagent to determine the remaining concentrations of Cr(VI) in each sample after adsorption at the desired time intervals. The analysis was carried out according to the procedure given by Gilcreas et al. [15]. The same procedure has been used to study the effect of initial concentration, pH, temperature and particle size. The pH was adjusted either with 0.1 M HCl or 0.1 M NaOH as required.

The equilibrium isotherm was determined by mixing 0.4 g of carbon with 50 ml of chromium solution in 125 ml conical flask at the required temperature. Each isotherm consisted of six chromium concentrations varied from 100 to 1000 ppm. The flasks containing chromium solution and carbon were placed in a shaker and agitated for 48 h at the required temperature and at a fixed agitation speed of 150 rpm. The equilibrium concentrations were measured by the spectrophotometer and referenced with the calibration curve.

The accuracy of temperature and concentration measurements was ±0.5°C and ±0.05 ppm, respectively.

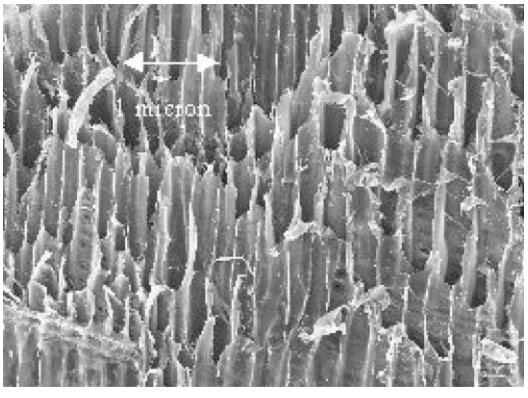

Fig. 4. SEM image of pyrolysed sawdust (SPC) sample.

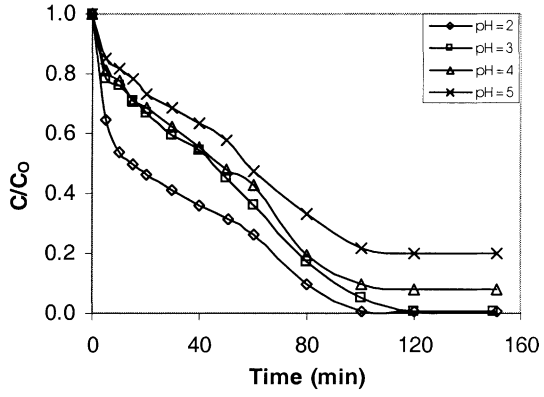

Fig. 5. Time variation of Cr(VI) adsorption on TAC at different pHs.

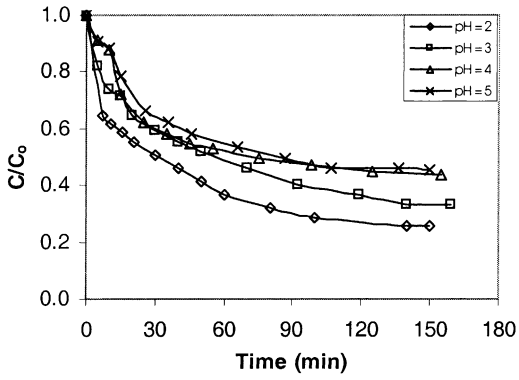

Fig. 6. Time variation of Cr(VI) adsorption on SPC at different pHs.

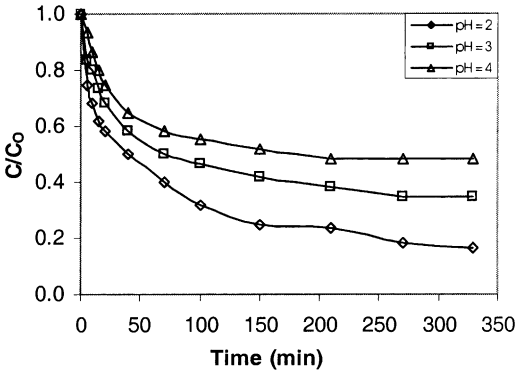

Fig. 7. Time variation of Cr(VI) adsorption on CAC at different pHs.

3. Results and discussions

3.1. Effect of pH

The uptakes of Cr(VI) by the three types of carbon (TAC, SPC and CAC) at different pHs at an initial concentration of 60 mg/l and a temperature of 22°C are shown in Figs. 5–7. For TAC and CAC, the particle sizes were 0.65 mm. For SPC, the particle size was 0.2 mm. For TAC, the amount adsorbed increases from 25.62 to 29.93 mg/g as the pH decreases from 5 to 2. While for SPC, the amount adsorbed increases from 20.09 to 24.646 mg/g as the pH decreases from 5 to 2. For CAC, the amount adsorbed increases from 19.13 to 26.25 mg/g as the pH decreases from 4 to 2. This indicates that the adsorption capacity of the adsorbent is clearly pH dependent. It is obvious that pH determines the extent of the Cr(VI) removal as well as providing a favourable adsorbent surface charge for the adsorption to occur.

Cr(VI) exists in different forms in aqueous solution and the stability of these forms is dependent on the pH of the system. The logarithmic concentration diagram for 10^{-3} M $H_2Cr_2O_4$ solution drawn by Benefield et al. [16] is shown in Fig. 8. This figure clearly indicates that out of various forms of Cr(VI), the $HCrO_4^-$ form is more stable in aqueous

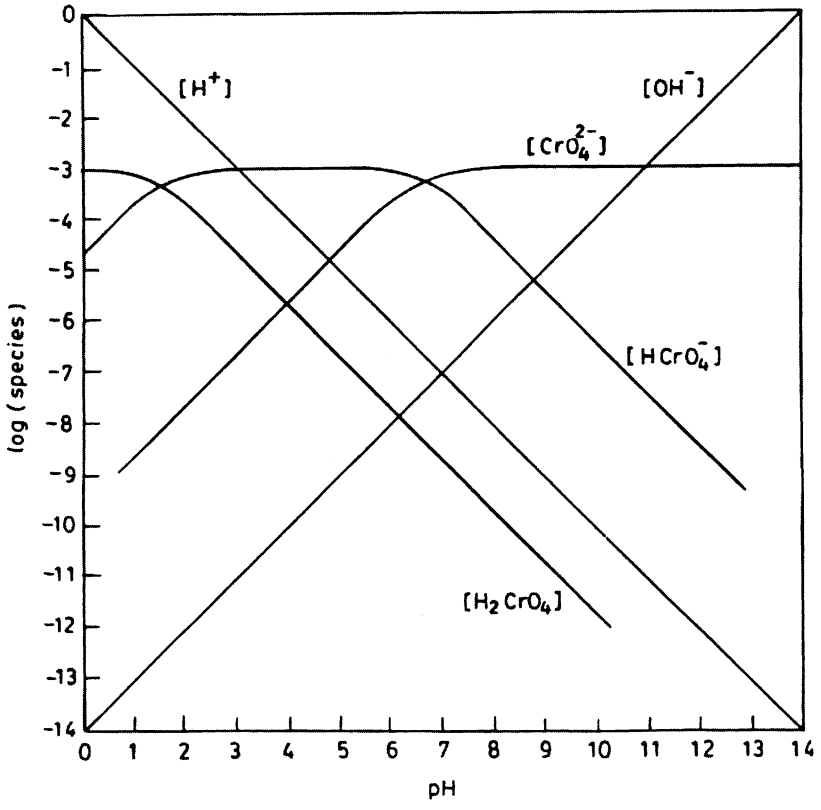

Fig. 8. Logarithmic concentration diagram for 10^{-3} M $H_2Cr_2O_4$ solution (adopted from [16]).

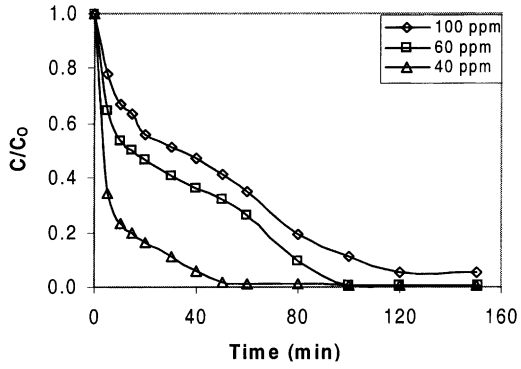

Fig. 9. Time variation of Cr(VI) adsorption on TAC at different initial concentrations.

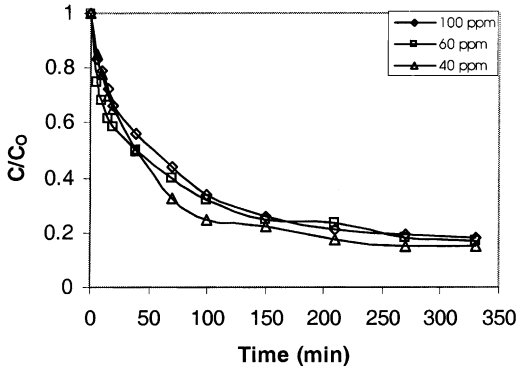

Fig. 11. Time variation of Cr(VI) adsorption on CAC at different initial concentrations.

solution up to pH = 7 beyond which it decreases. The H_2CrO_4 form is also stable within the low pH range, however, its concentration decreases sharply in aqueous solution with increasing pH. The CrO_4^{2-} form of Cr(VI) is stable in the higher pH range. Maximum adsorption at pH = 2 indicates that it is the $HCrO_4^-$ form of Cr(VI), which is the predominant species between pH = 1 and 4, which is adsorbed preferentially on the carbon.

3.2. Effect of initial concentration

The removal of Cr(VI) by adsorption on TAC and SPC has been shown to increase with time and attains a maximum value at about 120 min, and thereafter, it remains almost constant. On changing the initial concentration of Cr(VI) solution from 40 to 100 ppm, the amount adsorbed increases from 19.96 to 48.19 mg/g at 22°C, pH = 2 and average particle size of 0.65 mm for TAC (Fig. 9). While for CAC, the amount adsorbed increases from 17.75 to 43.25 mg/g (Fig. 10). For SPC at the same conditions with a particle size 0.2 mm, the amount adsorbed increases from 19.94 to 37.785 mg/g as the Cr(VI) concentration increases from 40 to 100 ppm (Fig. 11).

From Figs. 9–11, one can see that with lower initial concentration of adsorbate the amount of adsorbate attained on the solid phase is smaller than the amount attained when higher initial concentrations are used. However, the percentage removal of Cr(VI) for the TAC is similar with lower initial concentrations and with higher initial concentrations indicating that the activated carbon has an even greater adsorption power than the range of concentrations tested in this study. SPC, although its particle size is smaller, does not perform, as well as TAC. CAC appears not to be influenced by these initial concentrations and the process itself appears slower than for TAC.

3.3. Effect of particle size

Adsorption of Cr(VI) on TAC was found to decrease as the average particle size was increased from 0.38 to 0.9 mm. On changing the particle size from 0.38 to 0.9 mm (Fig. 12), the amount adsorbed increases from 27.74 to 29.93 mg/g at 22°C, pH = 2 and initial concentration of 60 mg/l. The relatively higher adsorption with smaller adsorbate particle may be attributed to the fact that smaller particles yield large surface areas. There is a tendency that smaller particles produce shorter time to equilibration.

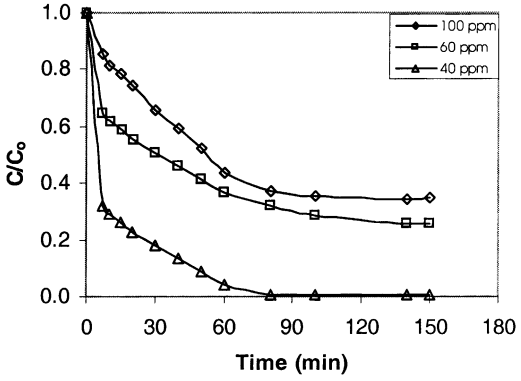

Fig. 10. Time variation of Cr(VI) adsorption on SPC at different initial concentrations.

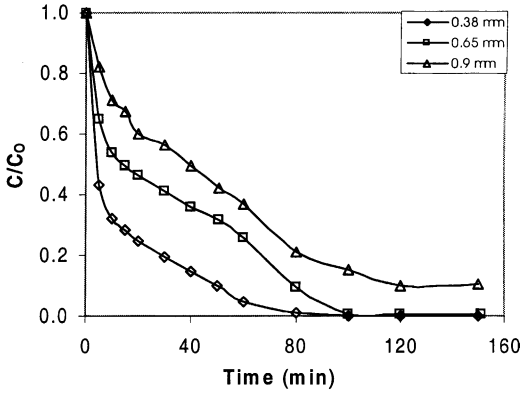

Fig. 12. Time variation of Cr(VI) adsorption on TAC at different particle sizes.

4. Adsorption kinetics modeling

The models of adsorption kinetics correlate the solute uptake rate, so these models are important in water treatment process design. In this study, for a batch reaction, the adsorption dynamics were followed by conducting the adsorption of Cr(VI) on adsorbent as described before.

4.1. First-order reversible reaction model

The sorption of chromium from liquid phase to solid may be considered as a reversible reaction with an equilibrium state being established between two phases [17]. A simple first-order reaction model was, therefore, used to correlate the rates of reaction, which can be expressed as

$$\mathrm{A} \underset{k_2}{\overset{k_1}{\rightleftarrows}} \mathrm{B} \tag{1}$$

If this model holds true, the rate equation for the reaction is expressed as

$$\frac{\mathrm{d}C_\mathrm{B}}{\mathrm{d}t} = -\frac{\mathrm{d}C_\mathrm{A}}{\mathrm{d}t} = k_1 C_\mathrm{A} - k_2 C_\mathrm{B} = C_{\mathrm{A}_0}\frac{\mathrm{d}X_\mathrm{A}}{\mathrm{d}t} = k_1(C_{\mathrm{A}_0} - C_{\mathrm{A}_0}X_\mathrm{A}) - k_2(C_{\mathrm{B}_0} - C_{\mathrm{A}_0}X_\mathrm{A}) \tag{2}$$

where C_B (mg/g) is the concentration of chromium on the sorbent and C_A (mg/l) the concentration of chromium in solution at any time, C_{B_0} and C_{A_0} the initial concentrations of chromium on sorbent and solution, respectively, X_A the fractional conversion of chromium and k_1 and k_2 are the first-order rate constants. At equilibrium conditions,

$$\frac{\mathrm{d}C_\mathrm{B}}{\mathrm{d}t} = -\frac{\mathrm{d}C_\mathrm{A}}{\mathrm{d}t} \tag{3}$$

and

$$X_{\mathrm{A}_\mathrm{e}} = \frac{K_\mathrm{c} - (C_{\mathrm{B}_0}/C_{\mathrm{A}_0})}{K_\mathrm{c} + 1} \tag{4}$$

where $X_{\mathrm{A}_\mathrm{e}}$ is the fractional conversion of chromium at equilibrium and K_c is the equilibrium constant defined as follows:

$$K_\mathrm{c} = \frac{C_{\mathrm{B}_\mathrm{e}}}{C_{\mathrm{A}_\mathrm{e}}} = \frac{C_{\mathrm{B}_0} - C_{\mathrm{A}_0}X_{\mathrm{A}_\mathrm{e}}}{C_{\mathrm{A}_0} - C_{\mathrm{A}_0}X_{\mathrm{A}_\mathrm{e}}} = \frac{k_1}{k_2} \tag{5}$$

where $C_{\mathrm{B}_\mathrm{e}}$ and $C_{\mathrm{A}_\mathrm{e}}$ are the equilibrium concentrations for chromium on the sorbent and solution, respectively. The rate equation in terms of equilibrium conversion can be obtained from Eqs. (2), (4) and (5)

$$\frac{\mathrm{d}X_\mathrm{A}}{\mathrm{d}t} = (k_1 + k_2)(X_{\mathrm{A}_\mathrm{e}} - X_\mathrm{A}) \tag{6}$$

Integration of Eq. (6) and substituting for k_2 from Eq. (5), gives

$$-\ln\left(1 - \frac{X_\mathrm{A}}{X_{\mathrm{A}_\mathrm{e}}}\right) = k_1\left(1 + \frac{1}{K_\mathrm{c}}\right)t \tag{7}$$

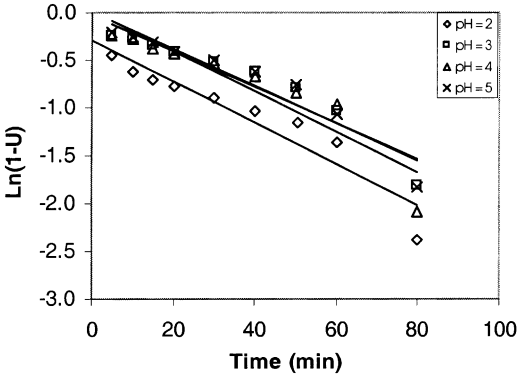

Fig. 13. First-order reversible reaction kinetics plot for adsorption of Cr(VI) on TAC at different pHs.

Thus, Eq. (7) can be rewritten in a different form

$$\ln[1 - U(t)] = -k_\mathrm{r}' t \tag{8}$$

where k_r' is the overall rate constant. Furthermore,

$$k_\mathrm{r}' = k_1\left(1 + \frac{1}{K_\mathrm{c}}\right) = k_1 + k_2 \tag{9}$$

and

$$U(t) = \frac{C_{\mathrm{A}_0} - C_\mathrm{A}}{C_{\mathrm{A}_0} - C_{\mathrm{A}_\mathrm{e}}} = \frac{X_\mathrm{A}}{X_{\mathrm{A}_\mathrm{e}}} \tag{10}$$

where $U(t)$ is called the fractional attainment of equilibrium. Plots for Eq. (8) were made for TAC, SPC and CAC at different pHs, at different initial concentrations, for different particle size and at different temperatures. Fig. 13 is shown as an example for these plots. Approximate linear fits were generally observed for all pHs, concentrations, particle size and temperatures indicating that sorption reaction can be approximated to be of the first-order reversible kinetics. Correlation coefficients were found to be between 0.8642 and 0.9982, which means that there is a good agreement but not a perfect one.

At $t = 0$, Eq. (8) yields $U(t) = 0$, connecting this point to the next data point resulted in the initial drop. To avoid any error that may be introduced in evaluating the rate constant due to this initial drop, the segments after the 'initial drop' were adopted for rate calculations. Arun and Venkobachar [17] and Michelsen et al. [18] also used this approach.

Constants k_1, k_2, k_r' and K_c were calculated using Eqs. (5) and (9) and are summarised in Tables 2–5.

4.2. Pseudo-first-order model

The sorption kinetics may also be described by a pseudo-first-order according to Ho and McKay [19] and Namasivayam and Kardivelu [20]

$$\frac{\mathrm{d}q}{\mathrm{d}t} = k_1'(q_\mathrm{e} - q) \tag{11}$$

Table 2
The first-order reversible reaction rate constants for the TAC, SPC and CAC at different pHs[a]

Sorbent	pH	k'_r (min^{-1})	k_1 (min^{-1})	k_2 (min^{-1})	K_c	r^2
TAC	2	0.0216	0.0215	0.0001	151.9340	0.8939
	3	0.0188	0.0186	0.0002	80.9377	0.9133
	4	0.0211	0.0180	0.0031	5.7574	0.8642
	5	0.0195	0.0133	0.0062	2.1211	0.9140
SPC	2	0.0243	0.0150	0.0093	1.6112	0.9893
	3	0.0208	0.0112	0.0096	1.1574	0.9937
	4	0.0275	0.0121	0.0154	0.7852	0.9615
	5	0.0298	0.0126	0.0172	0.7343	0.9906
CAC	2	0.0172	0.0125	0.0047	2.6250	0.993
	3	0.0128	0.0066	0.0062	1.0536	0.9838
	4	0.0177	0.0070	0.0107	0.6595	0.9766

[a] Temperature = 22°C, particle size = 0.65 mm, initial concentration = 60 mg/l.

Table 3
The first-order reversible reaction rate constants for the TAC, SPC and CAC at different initial concentrations[a]

Sorbent	C_0 (mg/l)	k'_r (min^{-1})	k_1 (min^{-1})	k_2 (min^{-1})	K_c	r^2
TAC	40	0.06351	0.0631	0.0004	166.3083	0.9359
	60	0.0216	0.0215	0.0001	151.9340	0.8939
	100	0.0236	0.0214	0.0022	9.6376	0.9310
SPC	40	0.037	0.0367	0.0003	124.6500	0.9488
	60	0.0243	0.0150	0.0093	1.6112	0.9893
	100	0.038	0.0198	0.0182	1.0827	0.9346
CAC	40	0.016	0.0120	0.0040	2.9583	0.9798
	60	0.011	0.0080	0.0030	2.6250	0.9698
	100	0.0147	0.0104	0.0043	2.4028	0.9984

[a] Temperature = 22°C, particle size = 0.65 mm, initial concentration = 60 m/l.

where q_e is the amount of solute adsorbed at equilibrium per unit weight of adsorbent (mg/g), q the amount of solute adsorbed at any time (mg/g) and k'_1 is the adsorption constant.

Eq. (11) is integrated for the boundary conditions $t = 0$ to >0 ($q = 0$ to >0) and then rearranged to obtain the following linear time dependence function:

$$\log(q_e - q) = \log(q_e) - \frac{k'_1}{2.303}t \quad (12)$$

Plots for Eq. (12) were made for TAC, SPC and CAC at different pHs, different initial concentrations, for different particle size and at different temperatures. Fig. 14 is shown as an example for these plots. Approximately, linear fits were observed for all pHs, concentrations, particle sizes and temperatures indicating that sorption reaction can be approximated to first-order kinetics. The smallest correlation coefficient in this case was 0.9288, which is still better than the first-order reversible reaction model. Constant k'_1 for all situations tested have been calculated and summarised in Tables 6–9.

Table 4
The first-order reversible reaction rate constants for the TAC for different particle sizes[a]

Sorbent	Particle size (mm)	k'_r (min^{-1})	k_1 (min^{-1})	k_2 (min^{-1})	K_c	r^2
TAC	0.38	0.043	0.0429	0.0001	499.63	0.9705
	0.65	0.0216	0.0215	0.0001	151.93	0.8939
	0.9	0.0262	0.0187	0.0075	2.50	0.9443

[a] Temperature = 22°C, initial concentration = 60 mg/l, pH = 2.

Table 5
The first-order reversible reaction rate constants for the TAC, SPC and CAC at different temperatures[a]

Sorbent	T (°C)	k'_r (min^{-1})	k_1 (min^{-1})	k_2 (min^{-1})	K_c	r^2
TAC	22	0.0216	0.0215	0.0001	151.93	0.8939
	30	0.0733	0.0729	0.0004	168.15	0.9301
	38	0.1594	0.1587	0.0007	212.38	0.9761
SPC	22	0.0243	0.0150	0.0093	1.61	0.9893
	30	0.0220	0.0173	0.0047	3.70	0.9618
	38	0.3520	0.3084	0.0436	7.08	0.9889
CAC	22	0.0172	0.0125	0.0047	2.63	0.9930
	30	0.0139	0.0118	0.0021	5.63	0.9975
	38	0.0142	0.0133	0.0009	14.63	0.9982

[a] Particle size = 0.65 mm, initial concentration = 60 mg/l, pH = 2.

4.3. Pseudo-second-order model

A pseudo-second-order model [19,21] may also describe the kinetics of sorption. The differential equation for this reaction is

$$\frac{dq}{dt} = k'_2(q_e - q)^2 \quad (13)$$

Integrating Eq. (13) for the boundary conditions $t = 0$ to >0 and $q = 0$ to >0 and rearranging to obtain the linearised form which is shown as follows:

$$\frac{t}{q} = \frac{1}{k'_2 q_e^2} + \frac{1}{q_e}t \quad (14)$$

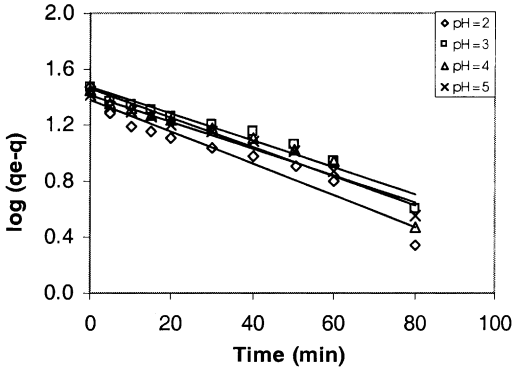

Fig. 14. First-order kinetics plot for adsorption of Cr(VI) on TAC at different pHs.

Table 6
The first-order reaction rate constants for the TAC, SPC and CAC at different pHs[a]

Sorbent	pH	k_1' (min^{-1})	r^2
TAC	2	0.0113	0.9288
	3	0.0095	0.9531
	4	0.0103	0.9223
	5	0.0095	0.9589
SPC	2	0.0127	0.9850
	3	0.0093	0.9890
	4	0.0104	0.9746
	5	0.0108	0.9905
CAC	2	0.0071	0.9807
	3	0.0055	0.9634
	4	0.0064	0.9763

[a] Temperature = 22°C, particle size = 0.65 mm, initial concentration = 60 mg/l.

Table 7
The first-order reaction rate constants for the TAC, SPC and CAC at different initial concentrations[a]

Sorbent	C_0 (mg/l)	k_1' (min^{-1})	r^2
TAC	40	0.0290	0.9810
	60	0.0113	0.9288
	100	0.0114	0.9595
SPC	40	0.0201	0.9257
	60	0.0115	0.9727
	100	0.0136	0.9810
CAC	40	0.0069	0.9975
	60	0.0050	0.9681
	100	0.0063	0.9975

[a] Temperature = 22°C, particle size = 0.65 mm, pH = 2.

Table 8
The first-order reaction rate constants for the TAC for different particle sizes[a]

Sorbent	Particle size (mm)	k_1' (min^{-1})	r^2
TAC	0.38	0.021	0.9755
	0.65	0.0113	0.9288
	0.90	0.0122	0.9688

[a] Temperature = 22°C, initial concentration = 60 mg/l, pH = 2.

Table 9
The first-order reaction rate constants for the TAC, SPC and CAC at different temperatures[a]

Sorbent	T (°C)	k_1' (min^{-1})	r^2
TAC	22	0.0113	0.9288
	30	0.0465	0.9598
	38	0.0752	0.9785
SPC	22	0.0127	0.9850
	30	0.0132	0.9796
	38	0.0111	0.9602
CAC	22	0.0071	0.9807
	30	0.0065	0.9859
	38	0.0067	0.9864

[a] Particle size = 0.65 mm, initial concentration = 60 mg/l, pH = 2.

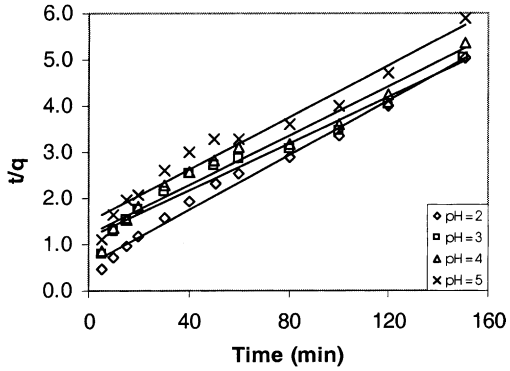

Fig. 15. Second-order reaction kinetics plot for adsorption of Cr(VI) on TAC at different pHs.

$$h = k_2' q_e^2 \quad (15)$$

In these equations, h is the initial sorption rate (mg/g min). The kinetics plots for Eq. (14) were made for TAC, SPC and CAC at different pHs, at different initial concentrations, for different particle sizes and at different temperatures. Fig. 15 is shown as an example for these plots. Good fits were observed for all pHs, concentrations, particle size and temperatures indicating that sorption reaction can be approximated with the second-order kinetics model. The smallest correlation coefficient in this case was 0.9579, which is even better than the first-order reaction model.

The constant k_2' is calculated from the figures and represented in Tables 10–13. It can be observed that h (the initial sorption rate, mg/g min) is generally higher for TAC than that of SPC and CAC.

5. Adsorption isotherm

The equilibrium data for adsorption of Cr(VI) on to the carbon sample may follow the rearranged Langmuir

Table 10
The second-order reaction rate constants for the TAC, SAC and CAC at different pHs[a]

Sorbent	pH	k_2' (g/mg min)	h (mg/g min)	r^2
TAC	2	0.0296	26.52	0.9864
	3	0.0253	22.57	0.9579
	4	0.0268	21.35	0.9612
	5	0.0283	18.58	0.9598
SPC	2	0.0369	22.41	0.9966
	3	0.0381	20.21	0.9969
	4	0.0411	17.31	0.9872
	5	0.0408	16.46	0.9966
CAC	2	0.0363	25.01	0.9990
	3	0.0424	20.76	0.9989
	4	0.0473	17.30	0.9975

[a] Temperature = 22°C, particle size = 0.65 mm, initial concentration = 60 mg/l.

Table 11
The second-order reaction rate constants for the TAC, SPC and CAC at different initial concentrations[a]

Sorbent	C_0 (mg/l)	k_2' (g/mg min)	h (mg/g min)	r^2
TAC	40	0.0488	19.44	0.9997
	60	0.0296	26.52	0.9864
	100	0.0173	40.17	0.9839
SPC	40	0.0481	19.13	0.9993
	60	0.0369	22.41	0.9969
	100	0.0205	29.27	0.9922
CAC	40	0.0516	16.26	0.9996
	60	0.0363	25.01	0.9980
	100	0.0211	39.47	0.9988

[a] Temperature = 22°C, particle size = 0.65 mm, pH = 2.

Table 12
The second-order reaction rate constants for the TAC for different particle sizes[a]

Sorbent	Particle size (mm)	k_2' (g/mg min)	h (mg/g min)	r^2
TAC	0.38	0.0310	27.86	0.9985
	0.65	0.0296	26.52	0.9864
	0.90	0.0292	7.11	0.9884

[a] Temperature = 22°C, initial concentration = 60 mg/l, pH = 2.

equation [22]:

$$\frac{C_e}{q_e} = \frac{1}{Q^0 b} + \frac{C_e}{Q^0} \quad (16)$$

where C_e is the equilibrium concentration (mg/l) and q_e the amount adsorbed at equilibrium (mg/g).

Figs. 16–18 indicate that the equilibrium concentration C_e of adsorbate in solution is higher at lower temperature and it decreases with increasing temperature, i.e. the adsorption is favoured at higher temperatures.

The Langmuir constants Q^0 and b, which are related to the adsorption capacity and heat of adsorption, respectively, were determined (Table 14) from the slope and intercepts of the linear plots of C_e/q_e versus C_e (Fig. 16 is shown as an example of these plots).

Table 13
The second-order reaction rate constants for the TAC, SPC and CAC at different temperatures[a]

Sorbent	T (°C)	k_2' (g/mg min)	h (mg/g min)	r^2
TAC	22	0.0296	26.52	0.9864
	30	0.0323	28.94	0.9992
	38	0.0330	29.59	0.9998
SPC	22	0.0369	22.41	0.9969
	30	0.0334	24.93	0.9952
	38	0.0329	26.98	0.9990
CAC	22	0.0377	25.98	0.9990
	30	0.0337	26.66	0.9983
	38	0.0324	27.72	0.9987

[a] Particle size = 0.65 mm, initial concentration = 60 mg/l, pH = 2.

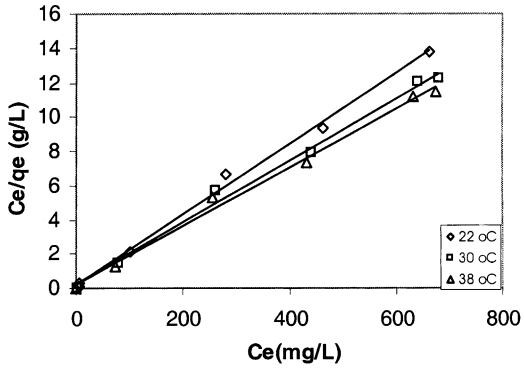

Fig. 16. Langmuir plots for the adsorption of Cr(VI) on TAC at different temperatures.

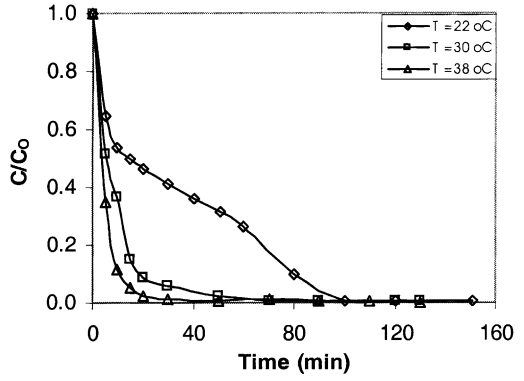

Fig. 17. Time variation of Cr(VI) adsorption on TAC at different temperatures.

5.1. The Gibb's free energies associated with the adsorption phenomena

The adsorption of Cr(VI) on SPC was found to increase from 24.65 to 28.64 mg/g when temperature was increased from 22 to 38°C (Fig. 18) at pH = 2, particle size of 0.2 mm and initial Cr(VI) concentration of 60 mg/l. For CAC, the adsorption of Cr(VI) was found to increase from 26.25 to 29.25 mg/g when temperature was increased from 22 to 38°C

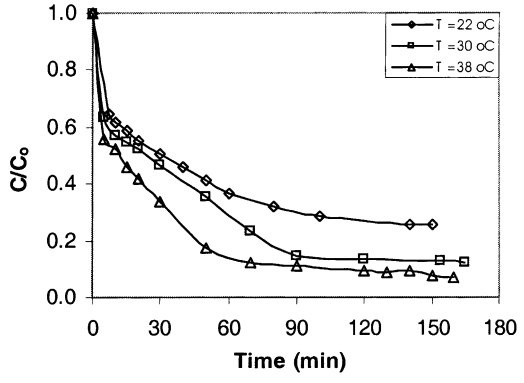

Fig. 18. Time variation of Cr(VI) adsorption on SPC at different temperatures.

Table 14
Langmuir constants for TAC, SPC and CAC samples at different temperatures[a]

Sorbent	T (°C)	Q^0	b	r^2
TAC	22	48.0769	0.1503	0.9969
	30	55.2486	0.0883	0.9935
	38	58.4795	0.0832	0.9928
SPC	22	1.9260	0.0252	0.9949
	30	2.1561	0.0278	0.9959
	38	2.2899	0.0281	0.9958
CAC	22	44.4444	0.0620	0.9951
	30	48.5437	0.0469	0.9949
	38	53.1915	0.0465	0.9938

[a] Particle size for TAC and CAC = 0.65 mm, particle size for TPC = 0.2 mm, pH = 2.

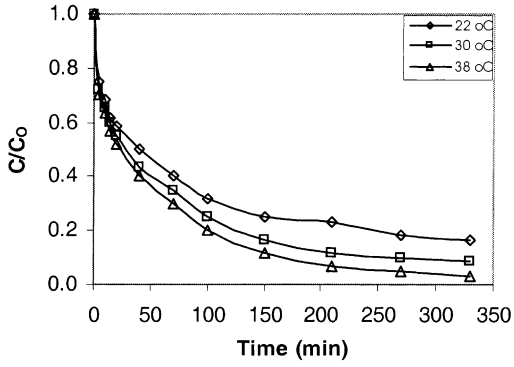

Fig. 19. Time variation of Cr(VI) adsorption on CAC at different temperatures.

(Fig. 19) at pH = 2, adsorbent particle size of 0.65 mm and initial Cr(VI) concentration of 60 mg/l. While for TAC, the final amount adsorbed has not been increased significantly but the rate of adsorption was greater at higher temperature (Fig. 17).

The increase in adsorption with a rise in temperature can be explained on the basis of thermodynamic parameters, i.e. the Gibb's free energy, which have been calculated using the following relationships according to Vinay and Prem [22]:

$$\Delta G^0 = -RT \ln K_c \quad (17)$$

The equilibrium constants K_c at different temperatures were estimated by the method described earlier in the first-order reversible reaction model. Table 15 summarises the results. The negative values of the free energy change (ΔG^0) at different temperatures indicate the spontaneous nature of adsorption. The adsorption is endothermic. This explains why the values of G^0 (Table 15) are negative and become lower with the rise in temperature.

Table 15
ΔG^0 (kJ/mol) for TAC, SPC and CAC

T (°C)	22	30	38
TAC	−12.33	−12.92	−13.86
SPC	−1.17	−3.30	−5.06
CAC	−2.37	−4.35	−6.94

6. Conclusions

In this paper, it has been shown that adsorbent materials derived through pyrolysis and activation, from waste carbonaceous materials like used tyres and sawdust can be manufactured. These adsorbents have been shown to have comparable performance to commercial activated carbon.

The results indicate that the optimum pH for the removal of Cr(VI) ions by TAC, SPC and CAC is around 2. The carbon produced from the used tyres is highly effective about (99% removal) at pH = 2, even at a low temperature of 22°C.

The temperature dependence is also evident from these experimental results. The sorption of Cr(VI) on TAC, SPC and CAC is endothermic. The pseudo-second-order chemical reaction model provides the best correlation of the data.

References

[1] P.T. Williams, S. Besler, D.T. Taylor, The pyrolysis of scarp automotive tyres, Fuel 69 (1990) 1474–1482.
[2] C. Roy, J. Unsworth, Pyrolysis and Gasification, Elsevier, London, UK, 1989.
[3] B.L. Schulman, P.A. White, Pyrolysis of used tyres using the Tosco II process — a progress report, in: J.L. Jones, S.B. Radding (Eds.), Solid Wastes and Residues: Conversion by Advanced Thermal Processes, American Chemical Society, Washington, DC, 1978.
[4] W. Kaminsky, H. Sinn, Pyrolysis of plastic waste and used tyres using fluidised bed process, in: J.L. Jones, S.B. Radding (Eds.), Thermal Conversion of Solid Wastes and Biomass, American Chemical Society, Washington, DC, 1980.
[5] W. Kaminsky, H. Rossler, Olefins from wastes, CHEMTECH 22 (1992) 108.
[6] A.A. Merchant, M.A. Petrich, Pyrolysis of used tyres and conversion of chars to activated carbon, AIChE J. 39 (8) (1993) 1370–1376.
[7] S.D. Faust, O.M. Aly, Adsorption Processes for Water Treatment, Butterworth Publishers, USA, 1987, 294 pp.
[8] G. McKay, M.J. Bino, A.R. Altamemi, The adsorption of various pollutants from aqueous solutions onto activated carbon, Water Res. 19 (4) (1985) 491–495.
[9] C. Selomulya, V. Meeyoo, R. Amal, Removal mechanism of Cr(VI) from wastewater by different types of activated carbons, CHEMECA'97, 1997.
[10] S.K. Ouki, R.D. Neufeld, Use of activated carbon for the recovery of chromium from industrial wastewater, J. Chem. Tech. Biotechnol. 70 (1997) 3–8.
[11] N.K. Hamadi, X.D. Chen, M.M. Farid, A.A. Makardij, G.Q. Lu, A batch removal of chromium(VI) from wastewater using cheap adsorbent materials, CHEMECA'98, Qld, Australia, 1998.
[12] N.K. Hamadi, X.D. Chen, M.M. Farid, G.Q. Lu, Activated carbon from used tyres as an adsorbent for colour removal from textile wastewater, CHEMECA'99, Newcastle, Australia, 1999.
[13] M.A. Wójtowicz, M.A. Serio, Pyrolysis of scrap tyres: can it be profitable? CHEMTECH (October 1996) 48–53.
[14] J.Y. Kim, J.K. Park, T.B. Edil, Sorption of organic compounds in the aqueous phase onto tyre rubber, J. Environ. Eng. 123 (1997) 827–835.

[15] F.W. Gilcreas, M.J. Tarars, R.S. Ingols, Standard Methods for the Examination of Water and Wastewater, 12th Edition, American Public Health Association, Inc., New York, 1965, p. 213.
[16] L.D. Benefield, J.F. Judkins Jr., B.L. Weand, Process Chemistry for Wastewater Treatment, Prentice-Hall, Englewood Cliffs, NJ, 1982, pp. 433–439.
[17] K. Arun, C. Venkobachar, Removal of cadmium(II) by low cost adsorbents, J. Environ. Eng. 110 (1984) 110–122.
[18] L.D. Michelsen, P.G. Gideon, E.G. Pace, L.H. Kutal, Removal of soluble mercury from wastewater by complexing techniques, U.S.D.I., Office of Water Research & Technology, Bull. No. 74, 1975.
[19] Y.S. Ho, G. McKay, Kinetic models for the sorption of dye from aqueous solution by wood, Trans. IChemE 76B (1998) 183–191.
[20] C. Namasivayam, K. Kardivelu, Uptake of mercury(II) from wastewater by activated carbon from an unwanted agricultural solid by-product, Carbon 37 (1999) 79–84.
[21] Y.S. Ho, G. McKay, Batch lead(II) removal from aqueous solution by peat equilibrium and kinetics, Trans. IChemE 77B (1999) 165–173.
[22] K.S. Vinay, N.T. Prem, Removal and recovery of chromium(VI) from industrial wastewater, J. Chem. Tech. Biotechnol. 69 (1997) 376–382.